# Enhanced Spontaneous and Benzo(*a*)pyrene-Induced Mutations in the Lung of Nrf2-Deficient *gpt* Delta Mice

Yasunobu Aoki,[1] Akiko H. Hashimoto,[1] Kimiko Amanuma,[1] Michi Matsumoto,[1] Kyoko Hiyoshi,[1,2] Hirohisa Takano,[1] Ken-ichi Masumura,[4] Ken Itoh,[3] Takehiko Nohmi,[4] and Masayuki Yamamoto[3]

[1]Research Center for Environmental Risk, National Institute for Environmental Studies; [2]Graduate School of Comprehensive Human Sciences; [3]Center for TARA and ERATO-JST, University of Tsukuba, Ibaraki, Japan; and [4]Division of Genetics and Mutagenesis, National Institute of Health Sciences, Tokyo, Japan

## Abstract

**The lung is an organ that is sensitive to mutations induced by chemicals in ambient air, and transgenic mice harboring guanine phosphoribosyltransferase (*gpt*) gene as a target gene are a well-established model system for assessing genotoxicity *in vivo*. Transcription factor Nrf2 mediates inducible and constitutive expression of cytoprotective enzymes against xenobiotics and mutagens. To address whether Nrf2 is also involved in DNA protection, we generated *nrf2*$^{+/-}$*::gpt* and *nrf2*$^{-/-}$*::gpt* mice. The spontaneous mutation frequency of the *gpt* gene in the lung was approximately three times higher in *nrf2*-null (*nrf2*$^{-/-}$) mice than *nrf2* heterozygous (*nrf2*$^{+/-}$) and wild-type (*nrf2*$^{+/+}$) mice, whereas in the liver, the mutation frequency was higher in *nrf2*$^{-/-}$ and *nrf2*$^{+/-}$ mice than in *nrf2*$^{+/+}$ wild-type mice. By contrast, no difference in mutation frequency was observed in testis among the three genotypes. A single intratracheal instillation of benzo(*a*)pyrene (BaP) increased the lung mutation frequency 3.1- and 6.1-fold in *nrf2*$^{+/-}$ and *nrf2*$^{-/-}$ mice, respectively, compared with BaP-untreated *nrf2*$^{+/-}$ mice, showing that *nrf2*$^{-/-}$ mice are more susceptible to genotoxic carcinogens. Surprisingly, mutation profiles of the *gpt* gene in BaP-treated *nrf2*$^{+/-}$ mice was substantially different from that in BaP-untreated *nrf2*$^{-/-}$ mice. In *nrf2*$^{-/-}$ mice, spontaneous and BaP-induced mutation hotspots were observed at nucleotides 64 and 140 of *gpt*, respectively. These results thus show that Nrf2 aids in the prevention of mutations *in vivo* and suggest that Nrf2 protects genomic DNA against certain types of mutations.** [Cancer Res 2007;67(12):5643–8]

## Introduction

Nrf2 is an essential transcription factor for inducible and constitutive expression of several phase II detoxification enzymes, including glutathione *S*-transferase-α (GST-α) and GST-π and UDP-glucuronosyl transferase 1A6 (1). Nrf2 also regulates the expression of antioxidant enzymes, including NAD(P)H:quinone oxidoreductase-1 and heme oxygenase-1, in response to oxidative stress (2, 3). Keap1 acts to harness Nrf2 to the cytoplasm, and Nrf2 in this complex rapidly undergoes ubiquitination and proteasomal degradation via Keap1-Cullin 3 E3 interactions (4). However, oxidative or electrophilic modification of Keap1 triggers Nrf2 stabilization (5, 6). During oxidative conditions, Nrf2 translocates into the nucleus and activates cytoprotective gene expression by heterodimerizing with small Maf family members and binding to antioxidant-responsive elements (ARE) or electrophile-responsive element in regulatory regions of cytoprotective genes.

Nrf2-mediated induction of cytoprotective enzymes plays an important role in mitigating the adverse effects of mutagens and oxidants. In Nrf2-deficient mice, which have attenuated basal and inducible expression of these enzymes (7): (*a*) DNA adduct formation is accelerated after diesel exhaust exposure (8); (*b*) hepatotoxicity is enhanced after acetaminophen administration (9); and (*c*) benzo(*a*)pyrene (BaP)–induced DNA adduct and neoplasm formation in forestomach is more prevalent than in wild-type mice (10, 11). Taken together, Nrf2 attenuation or malfunction may be an important aspect of diseases caused by environmental mutagens or oxidants, although the mechanism linking Nrf2 deficiency and mutation frequency is not well understood.

Transgenic guanine phosphoribosyltransferase (*gpt*) delta mice are a model system for detecting *in vivo* mutations (12). In this mouse system, the *gpt* gene is integrated into the genome as a target gene for detecting mutations, and when the *gpt* gene is rescued from genomic DNA to *Escherichia coli*, *gpt* mutants can be randomly selected as rescued *E. coli* colonies that form on plates containing 6-thioguanine (6-TG). To assess whether Nrf2 deficiency increases the mutational risk following exposure to BaP, the current study uses *nrf2*$^{-/-}$*::gpt* mice to analyze mutagenic activity *in vivo*. Furthermore, alterations in the mutation spectrum between *nrf2*$^{+/-}$ and *nrf2*$^{-/-}$ mice were assessed after exposure to BaP.

## Materials and Methods

**Mice.** C57BL/6J *nrf2* knockout mice (7) and *gpt* delta mice (C57BL/6J background; ref. 12) were as described previously, and *gpt* mice were obtained from Japan SLC. Nrf2-deficient mice (*nrf2*$^{-/-}$) were crossed with *gpt* delta transgenic mice (*nrf2*$^{+/+}$*::gpt/gpt*), and the resultant F1 mice (*nrf2*$^{+/-}$*::gpt/0*) were crossed again with Nrf2-deficient mice (*nrf2*$^{-/-}$) to produce *nrf2* knockout *gpt* mice that are homozygous (*nrf2*$^{-/-}$) or heterozygous (*nrf2*$^{+/-}$) to the *nrf2* knockout allele (*nrf2*$^{+/-}$*::gpt* and *nrf2*$^{-/-}$*::gpt*, respectively). Genotyping for *nrf2* was accomplished by PCR amplification of genomic DNA isolated from tails. PCR primers were as follows: 5′-TGGACGGGACTATTGAAGGCTG-3′ (sense for both genotype) and 5′-GCCGCCTTTTCAGTAGATGGAGG-3′ (antisense for wild-type mice) and 5′-GCGGATTGACCGTAATGGGATAGG-3′ (antisense for *LacZ*). The presence of the *gpt* transgene was confirmed by PCR as previously described (12). Nine male Nrf2-deficient *gpt* delta mice (*nrf2*$^{-/-}$*::gpt*) and nine male heterozygous *nrf2* knockout *gpt* delta mice (*nrf2*$^{+/-}$*::gpt*), both 7 to 9 weeks old, were obtained from this breeding scheme. Experiments

**Note:** Supplementary data for this article are available at Cancer Research Online (http://cancerres.aacrjournals.org/).

Y. Aoki and A.H. Hashimoto contributed equally to this work.

**Requests for reprints:** Yasunobu Aoki, National Institute for Environmental Studies, 16-2 Onogawa, Tsukuba, Ibaraki 305-8506, Japan. Phone: 81-29-850-2390; Fax: 81-29-850-2588; E-mail: ybaoki@nies.go.jp.



doi:10.1158/0008-5472.CAN-06-3355

were done according to protocols approved by the Institutional Animal Care and Use Committee at National Institute for Environmental Studies.

**Mouse treatment.** BaP (Wako Pure Chemical) was dissolved in tricaprylin $[CH_3(CH_2)_6COOCH_2]_2CHOCO(CH_2)_6CH_3$ (Sigma-Aldrich). Five *nrf2*$^{+/-}$*::gpt* mice and four *nrf2*$^{-/-}$*::gpt* mice were treated with 1 mg BaP dissolved in 50 μL tricaprylin given in a single intratracheal instillation under anesthesia with halothane for mutation analysis as previously reported (13). Vehicle (50 μL tricaprylin) was given to five *nrf2*$^{+/-}$*::gpt* mice and four *nrf2*$^{-/-}$*::gpt* mice as BaP-untreated groups. For immunoblot analysis, three *nrf2*$^{+/-}$ or *nrf2*$^{-/-}$ mice were used for each group. Mice were sacrificed 1 and 14 days after BaP administration under anesthesia with ethyl ether for Western blotting and mutation analysis, respectively. Lungs were removed, quickly frozen in liquid nitrogen, and stored at −80°C until the DNA was isolated.

***gpt* mutation assay.** Genomic DNA was extracted from the lungs using the RecoverEase DNA Isolation kit (Stratagene). Lambda EG10 phages were recovered from the genomic DNA using Transpack Packaging Extract (Stratagene). *E. coli* (YG6020 expressing Cre recombinase) were infected with the recovered phage harboring the *gpt* gene and the chloramphenicol (Cm) acethyltransferase (*cat*) gene (a selection marker), and these genes were rescued as a plasmid (14). The *gpt* mutants can be detected as colonies arising on plates containing Cm and 6-TG. The bacteria were then spread onto M9 salts plates containing Cm and 6-TG, which were incubated for 72 h at 37°C for selection of the colonies harboring a plasmid carrying a mutated *gpt* gene and *cat* gene. The 6-TG–resistant colonies were streaked onto selection plates for confirmation of the resistant phenotype. The cells were then cultured in Luria-Bertani broth containing 25 μg/mL of Cm at 37°C and collected by centrifugation. The bacterial pellets were stored at −80°C until DNA sequencing analysis was done. Mutant frequencies for the *gpt* gene were calculated by dividing the number of colonies growing on (M9 + Cm + 6-TG) agar plates by the number of colonies growing on (M9 + Cm) agar plates, which is the number of colonies harboring the plasmid. To ensure determination of the mutant frequency, mutant colonies were selected from over 300,000 colonies (15).

**PCR and DNA sequencing analysis of 6-TG–resistant mutants.** A 739-bp DNA fragment containing the *gpt* gene was amplified by PCR using primer 1 and primer 2, as described previously (13). The reaction mixture contained 5 pmol of each primer and 200 mmol/L of each deoxynucleotide triphosphate. PCR amplification was carried out using Ex Taq DNA polymerase (Takara Bio) and done with a Model PTC-100 Thermal Cycler (MJ Research). After the PCR products were purified, sequencing reactions were done by using a DYEnamic ET Terminator kit (Amersham Biosciences). The sequencing primers (primer A and primer C) were as described previously (13).

**Immunoblot analysis of GSTs.** Frozen lung was homogenized with 2 mL of 50 mmol/L HEPES buffer (pH 7.5) containing 150 mmol/L NaCl, 1 mmol/L DTT, and 0.2 mmol/L phenylmethylsulfonyl fluoride by glass-Teflon homogenizer chilled with ice. The homogenates were subjected to two steps of centrifugation at 4°C (15,000 × *g* for 15 min followed by 100,000 × *g* for 60 min) according to Chanas et al. (16). Resulting 100,000 × *g* supernatants (cytosol fractions) were stored at −80°C until use. After the cytosol fractions mixed with sample buffer containing 1% SDS were heated at 95°C, 9 μg protein ( for detecting GST A1/2) or 3 μg protein ( for detecting GST A3 and GST P1/2) from each sample was subjected to SDS-PAGE with 15% polyacrylamide gel (17). Proteins separated on the gel were transferred to Immobilon-P membrane (Amersham Biosciences). GST A1/2, GST A3 (18–20), and GST P1/2 were immunochemically detected using anti-mouse GST A1/2 and A3 rabbit sera (kindly provided by Dr. J.D. Hayes, University of Dundee, United Kingdom) and GST P1/2 rabbit serum (kindly provided by Dr. I. Hatayama, Aomori Prefecture Institute of Public Health and Environment, Japan), respectively, and goat anti-rabbit IgG antibody labeled with horseradish peroxidase (16). ECL-plus and Typhoon 9400 BioImage analyzer (Amersham Biosciences) were used to visualize bands.

**Statistical analysis.** All data are expressed as mean ± SD. Statistical significance of mutant frequency was evaluated using the Student's *t* test. $P < 0.05$ was considered statistically significant. Statistical comparisons of mutational spectra were done using the Adams-Skopek test (21).

## Results and Discussion

The frequency of spontaneous mutations in the lung, liver, and testis was compared among *gpt* delta mice (*nrf2*$^{+/+}$), heterozygous mice (*nrf2*$^{+/-}$), and homozygous mice (*nrf2*$^{-/-}$). In the lung and liver, the mutation frequency was significantly elevated in *nrf2*$^{-/-}$ mice, compared with *nrf2*$^{+/+}$ mice (Fig. 1*A*; Supplementary Table S1). The mutant frequency in the lung was approximately three times higher in *nrf2*$^{-/-}$ mice ($1.40 \pm 0.28 \times 10^{-5}$) than *nrf2*$^{+/-}$ and *nrf2*$^{+/+}$ mice ($0.48 \pm 0.05 \times 10^{-5}$ and $0.50 \pm 0.16 \times 10^{-5}$, respectively), whereas the mutant frequency was significantly higher in both *nrf2*$^{-/-}$ and *nrf2*$^{+/-}$ mice ($1.24 \pm 0.13 \times 10^{-5}$ and $1.47 \pm 0.15 \times 10^{-5}$, respectively) than *nrf2*$^{+/+}$ mice in liver ($0.72 \pm 0.24 \times 10^{-5}$). In contrast, no difference in mutation frequency was observed in testis among the three genotypes (Fig. 1*A*). Whereas

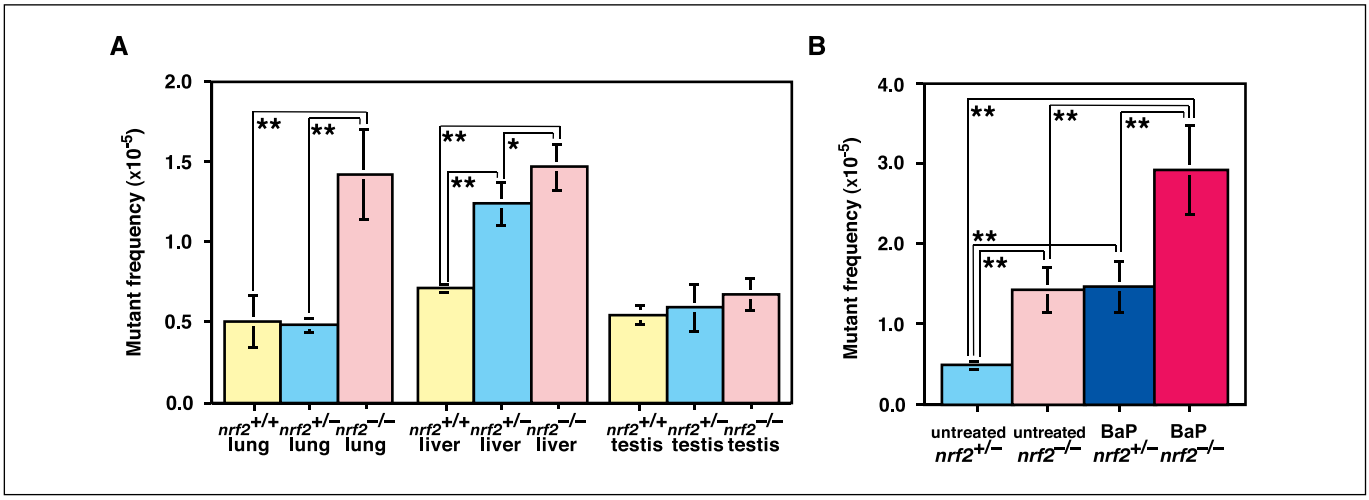


**Figure 1.** The mutant frequency of 6-TG selection (*A*) in the lung, liver, and testis of *gpt* delta mice (*nrf2*$^{+/+}$, *yellow column, n* = 3), and *nrf2*$^{+/-}$ (*light blue column, n* = 5) and *nrf2*$^{-/-}$ (*pink column, n* = 4) *gpt* delta mice and (*B*) in the lungs of *nrf2*$^{+/-}$ (*blue column, n* = 5) and *nrf2*$^{-/-}$ (*red column, n* = 4) *gpt* delta mice after BaP treatment. Data of *nrf2*$^{+/-}$ and *nrf2*$^{-/-}$ lungs in (*A*) are replicated as BaP-untreated *nrf2*$^{+/-}$ and *nrf2*$^{-/-}$, respectively, in (*B*). *Columns,* mean; *bars,* SD. *, $P < 0.05$; **, $P < 0.01$, statistical significance among the groups was determined using the Student's *t* test.

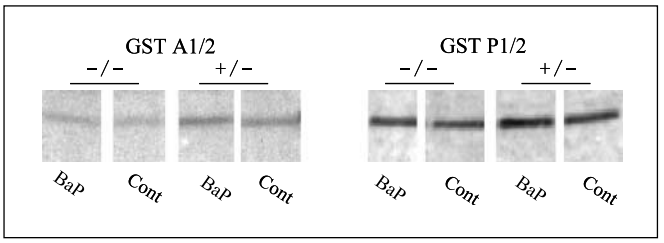


**Figure 2.** Immunodetection of GSTs. Cytosol fractions were extracted from the lungs of *nrf2*$^{+/-}$ (+/−) and *nrf2*$^{-/-}$ (−/−) mice, separated on SDS/PAGE, and electrophoretically blotted to Immobilon-P membrane. GST A1/2 and GST P1/2 were detected immunochemically using specific antibodies and ECL-plus system. BaP, cytosol fractions extracted from BaP-treated mouse lungs; *Cont,* cytosol fractions extracted from BaP-untreated mouse lungs.

the DNA repair system is quite efficient in the testis (22), metabolically active tissues, such as the liver and lung, seem to be unable to efficiently repair the DNA adducts produced by reactive oxygen species and/or endogenous mutagens without the presence of Nrf2. These results suggest that Nrf2 acts to suppress spontaneous mutagenesis in the lung and liver.

We aimed to quantitatively determine how Nrf2 deficiency affects mutagenicity *in vivo* in the lung using a single intratracheal instillation of BaP as a model environmental mutagen/carcinogen (13). BaP in cigarette smoke or ambient air is readily oxidized to reactive intermediates, such as BaP diol epoxide, by phase I detoxifying enzymes (23), and these intermediates are subsequently metabolized to hydrophilic conjugates by phase II detoxifying enzymes that are under Nrf2 regulation. However, unconjugated reactive intermediates, which often form, lead to DNA adduct formation (24). DNA adducts cause mispairing of DNA bases and induce gene mutations through the DNA replication process (25, 26). This process has been confirmed by *in vitro* experiment using BaP adduct-containing DNA as a template (27, 28). Indeed, a single intratracheal instillation of BaP into *gpt* delta mice resulted in a statistically significant and dose-dependent increase in the mutant frequency in the lungs of *gpt* delta mice, and the most frequent mutation induced by BaP was G:C to T:A transversion (13), which is characteristic of BaP mutagenesis (25, 26).

Therefore, *nrf2*$^{-/-}$*::gpt* and *nrf2*$^{+/-}$*::gpt* mice were given a carcinogenic dose (1 mg; ref. 29) of BaP through trachea, which resulted in a significant increase in the mutation frequency in lungs of both *nrf2*$^{+/-}$ and *nrf2*$^{-/-}$ mice. Importantly, BaP-treated *nrf2*$^{-/-}$ mice had a 2-fold higher mutant frequency ($2.93 \pm 0.56 \times 10^{-5}$) than BaP-treated *nrf2*$^{+/-}$ mice ($1.47 \pm 0.31 \times 10^{-5}$; Fig. 1*B*; Supplementary Table S2). The increment of mutant frequency by BaP treatment was higher in *nrf2*$^{-/-}$ mice than in *nrf2*$^{+/-}$ mice.

We thought that the expression level of Nrf2-regulated cytoprotective enzymes may explain both the higher basal mutant frequency in the Nrf2-deficient mouse and that following treatment of Nrf2-deficient mouse with BaP. Because Chanas et al. have shown that the class π GST isozymes are expressed at substantially lower levels in the livers of Nrf2-deficient mice than in wild-type mice (16). Because a thorough study of pulmonary GSTs in Nrf2-deficient mice has not been described in the literature, we decided to examine whether expression of GSTs was actually suppressed in the lungs of BaP-treated and BaP-untreated *nrf2*$^{-/-}$ mice by immunoblotting. In this study, we have examined expression of GST A1/2, GST A3, and GST P1/2, as these GSTs are known to be under the regulation of the Nrf2-ARE system (7) and are essential for the detoxification of BaP (30). Showing very good agreement with the report by Chanas et al. (16), which analyzed the expression of these enzymes in the mouse livers, the expression level of GST A1/2 was suppressed in the lungs of *nrf2*$^{-/-}$ mice compared with that in the *nrf2*$^{+/-}$ mice (Fig. 2), and the level of GST A3 was also low in Nrf2-deficient mice (data not shown). Under the experimental condition, GST A1/2 level was not elevated substantially by the BaP treatment in the lungs of *nrf2*$^{+/-}$ mice. Similarly, the expression level of GST P1/2 was also suppressed in the lungs of *nrf2*$^{-/-}$ mice compared with that in the *nrf2*$^{+/-}$ mice. GST P1/2 level was elevated by the BaP treatment in the lung of *nrf2*$^{+/-}$ mice, but there was no such difference in *nrf2*$^{-/-}$ mice. As the change in this immunoblotting experiment was relatively small, we repeated this experiment and found that the result was reproducible (data not shown). These results thus suggest that Nrf2 keeps the mutation frequency at low level in the lungs of mice by directing the expression the GSTs. As the changes in this GST immunoblotting experiments was relatively small, we speculate that lack of the

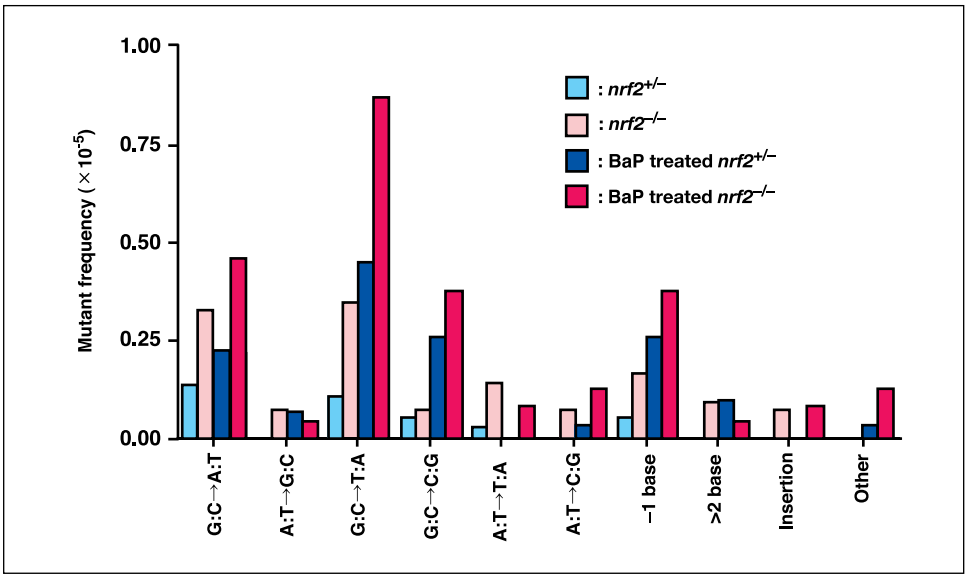


**Figure 3.** Comparison of mutant frequencies among the types of mutations in BaP-treated and BaP-untreated *nrf2*$^{+/-}$ and *nrf2*$^{-/-}$ mice. *Light blue column,* BaP-untreated *nrf2*$^{+/-}$ mice; *pink column,* BaP-untreated *nrf2*$^{-/-}$ mice; *blue column,* BaP-treated *nrf2*$^{+/-}$ mice; *red column,* BaP-treated *nrf2*$^{-/-}$ mice.

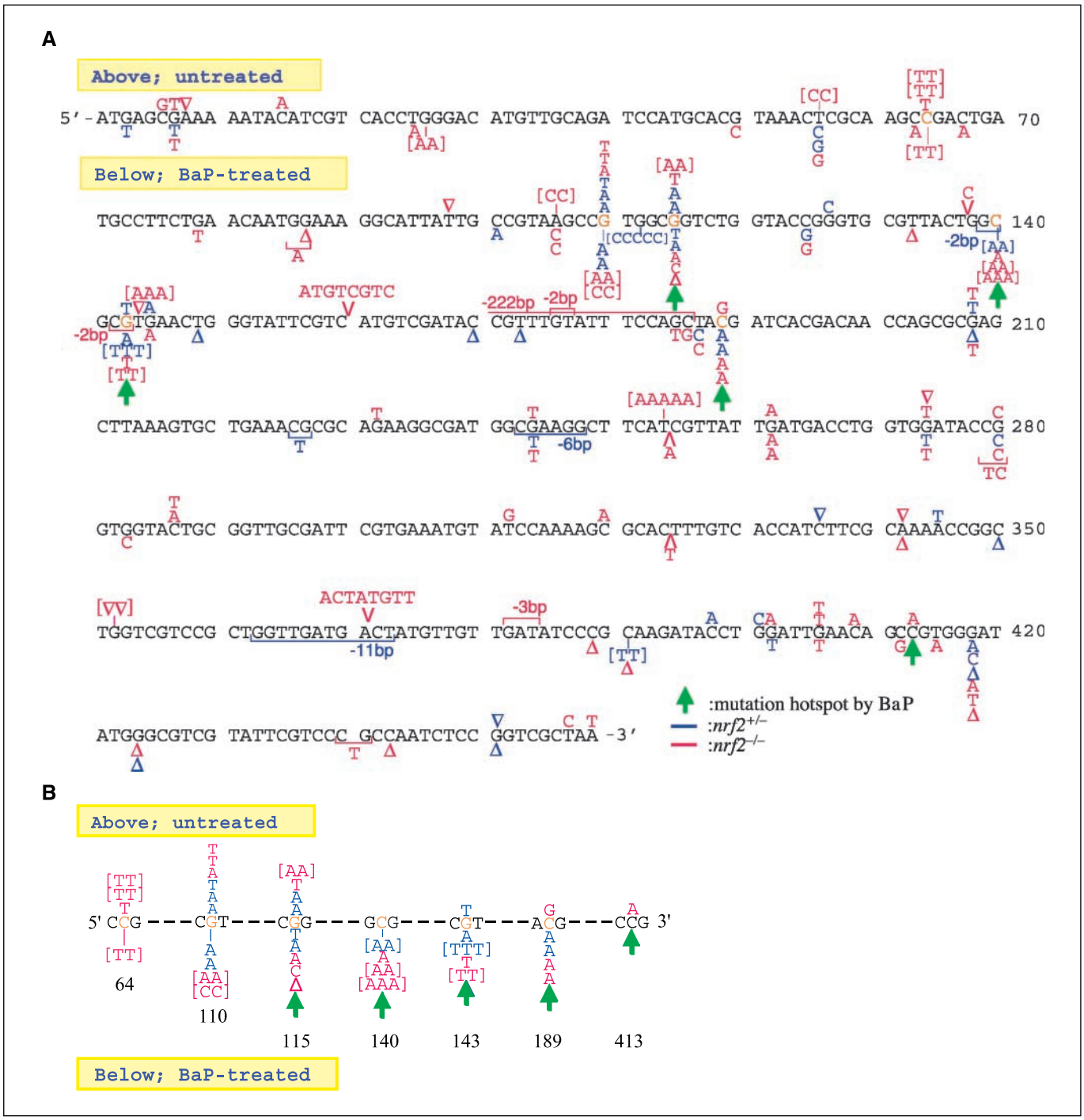


**Figure 4.** Overall distribution of the mutation detected on the *gpt* gene in the lungs of BaP-treated *nrf2*$^{+/-}$ and *nrf2*$^{-/-}$ mice and BaP-untreated *nrf2*$^{+/-}$ and *nrf2*$^{-/-}$ mice. The mutations are summarized in Supplementary Table S4. *A,* Mutations detected in *nrf2*$^{+/-}$ (*blue*) and *nrf2*$^{-/-}$ (*pink*) mice. The mutations detected in BaP-treated (*below* gpt *sequence*) and BaP-untreated mice (*above* gpt *sequence*). The number of characters in parenthesis is the number of mutations in one mouse. *Δ,* one base deletion; *half-boxes,* deleted nucleotides; *V,* a position of insertion. *Green arrows,* guanine nucleotides of BaP-induced mutation hotspots reported previously (13); *orange characters,* mutation hotspots found in this study. *B,* close-up of hotspots of mutations.

other Nrf2 target genes may also contribute to the mutant frequency in Nrf2-deficient mice.

To further characterize the mutational profile in the lungs of *nrf2*$^{-/-}$*::gpt* and *nrf2*$^{+/-}$*::gpt* mice after BaP exposure, we did DNA sequence analysis of 178 *gpt* mutant lung samples (Fig. 3; Supplementary Table S3). In *nrf2*$^{-/-}$ mice, the predominant spontaneous mutations were G:C to T:A transversion (26%, 15 of 58), G:C to A:T transition (24%, 14 of 58), and base deletions (19%, 11 of 58; Supplementary Table S3). A previous report of *gpt* delta mice (*mmh/ogg1*::*gpt*) suggested that accumulation of 8-hydroxyguanine in cells was the primary cause of increase in G:C to T:A transversion (31). 8-Hydroxyguanine may also play a role in the

induction of G:C to T:A transversion in the lungs of *nrf2*$^{-/-}$ mice because the level of antioxidant enzymes were suppressed in *nrf2*$^{-/-}$ mice, and subsequently, generation of reactive oxygen spices was probably accelerated.

The BaP treatment increased base substitutions at G:C pairs and one base deletion both in *nrf2*$^{+/-}$ and *nrf2*$^{-/-}$ mice (Fig. 3). Among the G:C substitutions, G:C to T:A and G:C to C:G transversions were markedly elevated in *nrf2*$^{-/-}$ mice after BaP treatment. Consistent with our previous studies with *gpt* delta mice (13), the predominant mutation provoked by BaP treatment was a G:C to T:A transversion (a major base substitute induced by the BaP-DNA adduct formation) in both *nrf2*$^{+/-}$ (32%, 14 of 44) and *nrf2*$^{-/-}$ (34%, 21 of 62) mice (Supplementary Table S2), and the mutant frequency of this transversion was higher in BaP-treated *nrf2*$^{-/-}$ mice than BaP-treated *nrf2*$^{+/-}$ mice (Fig. 3). In the lungs of *nrf2*$^{-/-}$ mice, DNA adducts are probably accumulated in the higher level than those in *nrf2*$^{+/-}$ mice because the expression levels of phase II enzymes that detoxify BaP by forming conjugates (32) and antioxidant enzymes are low in *nrf2*$^{-/-}$ mice comparing to *nrf2*$^{+/-}$ mice. We surmise that this increase of DNA adduct formation might elevate the mutant frequency of G:C to T:A transversion in the Nrf2-deficient condition. Additionally, generation of oxidative DNA adduct due to BaP-derived quinines (33) may be accelerated in *nrf2*$^{-/-}$ mice and play a role, albeit partly, in elevating the mutant frequency in *nrf2*$^{-/-}$ mice. Indeed, BaP adduct formation was accelerated ~2-fold in Nrf2-deficient mouse forestomach compared with wild-type mice (11), supporting our contention that the increase in the amount of DNA adduct enhanced the frequency of these transversions at G:C pairs.

To delineate the mode of mutation in Nrf2-deficient mice, the mutation positions in the *gpt* gene of BaP-treated and BaP-untreated mice were determined (Fig. 4*A*; Supplementary Table S4). Of the mutations found in BaP-treated mice (shown in lower side of the *gpt* sequence; Fig. 4*A*), G:C to T:A transversions at nucleotides 140, 143, and 189 were observed in three or more mice, including both *nrf2*$^{+/-}$ and *nrf2*$^{-/-}$ mice. Thus, these nucleotides are the hotspots of BaP-induced mutation. These nucleotides coincide with those previously reported (i.e., nucleotides 115, 140, 143, 189, and 413; ref. 13), which are shown with green arrows in Fig. 4*A*. The frequency of mutation at these hotspots was rather low in BaP-untreated mice (shown in upper side of the *gpt* sequence; Fig. 4*A*).

Because mutations were accumulated at relatively high level in the *gpt* gene of *nrf2*$^{-/-}$ mice even without BaP treatment, we assumed that we could assess hotspots of spontaneous mutation in these mice. Indeed, G:C to A:T transition at nucleotides 64 was observed in three BaP-untreated mice and one BaP-treated mouse. This mutation is exclusive in *nrf2*$^{-/-}$ mice. Thus, nucleotide 64 is the spontaneous mutation hotspot in Nrf2-deficient condition. In contrast, nucleotides 110 and 115 are common hotspots in BaP-treated and BaP-untreated mice; G:C to A:T transition at position 110 was observed in three BaP-untreated and three BaP-treated mice, and G:C to T:A transversion was also induced in three BaP-untreated mice.

Figure 4*B* shows mutation hotspots in the *gpt* gene. We found that one of the major trinucleotide sequences with BaP-induced guanine nucleotide mutation in this gene was CGT (nucleotides 110, 143, and 189). This is in good agreement with the previous observation that the instillation of BaP into the lung of *gpt* delta mice induced mutations frequently in CGT trinucleotide of the gene (13). CGG (nucleotides 64, 115, and 413) was another frequently found trinucleotide with guanine nucleotide mutations, but no link was found between this mutation and BaP treatment. It should be noted that guanine centered in CGC at position 140 was a frequent target of BaP-induced mutation in Nrf2-deficient condition, whereas previous experiments showed mutations were little in CGC of wild-type mice (13).

Whereas there was no significant difference in the mutation frequency, the position of the mutation was significantly different between BaP-untreated *nrf2*$^{-/-}$ mice and BaP-treated *nrf2*$^{+/-}$ mice (Fig. 4*A*; $P < 0.05$, Adams-Skopek test). This result suggests that chemical mutagenesis and spontaneous mutation in the *nrf2*$^{-/-}$ mice arise through different mechanisms. Thus, the Nrf2 deficiency had a marked affect on the mutational profile that arose either spontaneously or by BaP induction. However, further studies are required to clarify how Nrf2 deficiency alters the mutation profile, and whether nucleotides surrounding the guanine nucleotide are important for the mutation frequency in BaP-treated mice and in BaP-untreated *nrf2*$^{-/-}$ mice.

Several lines of recent evidence have pointed towards a role for Nrf2 in prevention of carcinogenesis. One of the salient examples is that Nrf2 could prevent the formation of DNA adduct and gastric tumors from occurring after BaP administration (10, 11). Furthermore, Nrf2-deficient mice are sensitive to the alkylating agent [*N*-nitrosobutyl(4-hydrixybutyl)amine] and rapidly form bladder tumors after administration (34). This study shows that Nrf2 can prevent increase in the number of spontaneous and inducible mutations that occur in the *gpt* gene in mouse lung and liver and can prevent the induction of mutations at the hotspots, such as nucleotides 64 and 140 in the lung. We surmise that through induction of phase II and antioxidant enzyme activities as well as cross-talk with phase I detoxifying system (35), Nrf2 can mitigate the effects of mutagens, such as BaP, on adduct formation, leading to protection from neoplasm and tumor formation and ultimately aiding in prevention of pulmonary diseases that arise, such as lung cancer from tobacco smoke (36), or from hyperoxic injury (37).

The results presented in this study suggest that Nrf2 deficiency is a possible risk factor for development of lung cancer or other lung diseases caused by mutagens or oxidants in ambient air. Whereas molecular mechanisms by which Nrf2 deficiency changes the mutation profile still require clarification, one plausible explanation is that Nrf2 deficiency may allow accumulation of specific reactive oxygen intermediates or electrophiles. We are now examining how exaggerated mutagenesis in the Nrf2-deficient condition quantitatively contributes to the enhanced carcinogenicity. We believe that the Nrf2-deficient *gpt* delta mice will provide useful information for revealing the relationship between *in vivo* mutagenesis and carcinogenicity.

## Acknowledgments

Received 9/18/2006; revised 3/10/2007; accepted 4/9/2007.

**Grant support:** Japan Society for the Promotion of Sciences grant-in-aid for scientific research 14207100 (Y. Aoki, A.H. Hashimoto, T. Nohmi, and M. Yamamoto) and JST-ERATO (K. Itoh and M. Yamamoto).

The costs of publication of this article were defrayed in part by the payment of page charges. This article must therefore be hereby marked *advertisement* in accordance with 18 U.S.C. Section 1734 solely to indicate this fact.

We thank Dr. John D. Hayes for providing us anti-mouse GST A1/2 and GST A3 antibodies; Dr. Ichiro Hatayama for GST P1/2 antibody; Drs. Hiroaki Shiraishi, Wakae Maruyama, Rie Yanagisawa (National Institute for Environmental Studies), and Jon Maher (University of Tsukuba) for their support and advice; and Yukari Sakashita, Yoshiki Sugawara (National Institute for Environmental Studies), and Katsuyoshi Hayashi (Animal Care Co., Ltd.) for their excellent technical contribution.

## References


1. Motohashi H, Yamamoto M. Nrf2-Keap1 defines a physiologically important stress response mechanism. Trends Mol Med 2004;10:549–57.
2. Ishii T, Itoh K, Takahashi S, et al. Transcription factor Nrf2 coordinately regulates a group of oxidative stress-inducible genes in macrophages. J Biol Chem 2000;275:16023–9.
3. Cho HY, Jedlicka AE, Reddy SP, et al. Role of NRF2 in protection against hyperoxic lung injury in mice. Am J Respir Cell Mol Biol 2002;26:175–82.
4. Tong KI, Kobayashi A, Katsuoka F, Yamamoto M. Two-site substrate recognition model for Keap1-Nrf2 system: a hinge and latch mechanism. Biol Chem 2006;387:1311–20.
5. Itoh K, Tong KI, Yamamoto M. Molecular mechanism activating Nrf2-Keap1 pathway in regulation of adaptive response to electrophiles. Free Radic Biol Med 2004;36:1208–13.
6. Kobayashi A, Kang MI, Watai Y, et al. Oxidative and electrophilic stresses activate Nrf2 through inhibition of ubiquitination activity of Keap1. Mol Cell Biol 2006;26:221–9.
7. Itoh K, Chiba T, Takahashi S, et al. An Nrf2/small Maf heterodimer mediates the induction of phase II detoxifying enzyme genes through antioxidant response elements. Biochem Biophys Res Commun 1997;236:313–22.
8. Aoki Y, Sato H, Nishimura N, Takahashi S, Itoh K, Yamamoto M. Accelerated DNA adduct formation in the lung of the Nrf2 knockout mouse exposed to diesel exhaust. Toxicol Appl Pharmacol 2001;173:154–60.
9. Enomoto A, Itoh K, Nagayoshi E, et al. High sensitivity of Nrf2 knockout mice to acetaminophen hepatotoxicity associated with decreased expression of ARE-regulated drug metabolizing enzymes and antioxidant genes. Toxicol Sci 2001;59:169–77.
10. Ramos-Gomez M, Kwak MK, Dolan PM, et al. Sensitivity to carcinogenesis is increased and chemoprotective efficacy of enzyme inducers is lost in nrf2 transcription factor-deficient mice. Proc Natl Acad Sci U S A 2001;98:3410–5.
11. Ramos-Gomez M, Dolan PM, Itoh K, Yamamoto M, Kensler TW. Interactive effects of nrf2 genotype and oltipraz on benzo[*a*]pyrene-DNA adducts and tumor yield in mice. Carcinogenesis 2003;24:461–7.
12. Nohmi T, Katoh M, Suzuki H, et al. A new transgenic mouse mutagenesis test system using Spi- and 6-thioguanine selections. Environ Mol Mutagen 1996;28:465–70.
13. Hashimoto AH, Amanuma K, Hiyoshi K, et al. *In vivo* mutagenesis induced by benzo[*a*]pyrene instilled into the lung of *gpt* delta transgenic mice. Environ Mol Mutagen 2005;45:365–73.
14. Nohmi T, Suzuki T, Masumura K. Recent advances in the protocols of transgenic mouse mutation assays. Mutat Res 2000;455:191–215.
15. Thybund V, Dean S, Nohmi T, et al. *In vivo* transgenic mutation assays. Mutat Res 2003;540:141–51.
16. Chanas SA, Jiang G, McMahon M, et al. Loss of the Nrf2 transcription factor causes a marked reduction in constitutive and inducible expression of the glutathione *S*-transferase *Gsta1, Gsta2, Gstm1, Gstm2, Gstm3* and *Gstm4* genes in the liver of male and female mice. Biochem J 2002;365:405–18.
17. Aoki Y, Satoh K, Sato K, Suzuki KT. Induction of glutathione S-transferase P-form in primary cultured rat liver parenchymal cells by co-planar polychlorinated biphenyl congeners. Biochem J 1992;281:539–43.
18. McLellan LI, Hayes JD. Differential induction of class alpha glutathione *S*-transferases in mouse liver by the anticarcinogenic antioxidant butylated hydroxyanisole. Purification and characterization of glutathione *S*-transferase Ya1Ya1. Biochem J 1989;263:393–402.
19. Hayes JD, Judah DJ, Neal GE, Nguyen T. Molecular cloning and heterologous expression of a cDNA encoding a mouse glutathione *S*-transferase Yc subunit possessing high catalytic activity for aflatoxin B1-8,9-epoxide. Biochem J 1992;285:173–80.
20. Hayes JD, Flangan JU, Jowsey IR. Glutathione transferase. Annu Rev Pharmacol Toxicol 2005;25:51–88.
21. Cariello NF, Piegorsch WW, Adams WT, Skopek TR. Computer program for the analysis of mutational spectra: application to p53 mutations. Carcinogenesis 1994;15:2281–5.
22. Tomascik-Cheeseman LM, Colemana MA, Marchettia F, et al. Differential basal expression of genes associated with stress response, damage control, and DNA repair among mouse tissues. Mutat Res 2004;561:1–14.
23. Buening MK, Wislocki PG, Levin W, et al. Tumorigenicity of the optical enantiomers of the diastereomeric benzo[*a*]pyrene 7,8-diol-9,10-epoxides in newborn mice: exceptional activity of (+)-7beta,8alpha-dihydroxy-9alpha,10alpha-epoxy-7,8,9,10-tetrahydrobenzo[*a*]pyrrene. Proc Natl Acad Sci U S A 1978;75:5358–61.
24. Cosman M, de los Santos C, Fiala F, et al. Solution conformation of the major adduct between the carcinogen (+)-anti-benzo[*a*]pyrene diol epoxide and DNA. Proc Natl Acad Sci U S A 1992;89:1914–8.
25. Hakura A, Tsutsui Y, Sonoda J, Tsukidate K, Mikami T, Sagami F. Comparison of the mutational spectra of the *lacZ* transgene in four origins of the Muta Mouse treated with benzo[*a*]pyrene: target organ specificity. Mutat Res 2000;447:239–47.
26. Shane BS, de Boer J, Watson DE, Haseman JK, Glickman BW, Tindall KR. *LacI* mutation spectra following benzo[*a*]pyrene treatment of Big Blue mice. Carcinogenesis 2000;21:715–25.
27. Hanrahan CJ, Bacolod MD, Vyas RR, et al. Sequence specific mutagenesis of the major (+)-anti-benzo[*a*]pyrene diol epoxide-DNA adduct at a mutational hot spot *in vitro* and in *Escherichia coli* cells. Chem Res Toxicol 1997;10:369–77.
28. Chiapperino D, Kroth H, Kramarczuk IH, et al. Preferential misincorporation of purine nucleotides by human DNA polymerase eta opposite benzo[*a*]pyrene 7,8-diol 9,10-epoxide deoxyguanosine adducts. J Biol Chem 2002;277:11765–71.
29. Yoshimoto T, Inoue T, Iizuka H, et al. Differential induction of squamous cell carcinoma and adenocarcinoma on mouse lung by intratracheal instillation of benzo(a)pyrene and charcoal powder. Cancer Res 1980;40:4301–7.
30. Dreij K, Sundberg K, Johansson AS, et al. Catalytic activities of human alpha class, glutathione transferases toward carcinogenic dibenzo[*a l*]pyrene diol epoxides. Chem Res Toxicol 2002;15:825–31.
31. Arai T, Kelly VP, Komoro K, Minowa O, Noda T, Nishimura S. Cell proliferation in liver of *mmh/ogg1*-deficient mice enhances mutation frequency because of the presence of 8-hydroxyguanine in DNA. Cancer Res 2003;63:4287–92.
32. Srivastava SK, Watkins SC, Schuetz E, Singh SV. Role of glutathione conjugate efflux in cellular protection against benzo[*a*]pyrene-7,8-diol-9,10-epoxide-induced DNA damage. Mol Carcinog 2002;33:156–62.
33. Burdick AD, Davis JW II, Liu KJ, et al. Benzo[*a*]pyrene quinones increase cell proliferation, generate reactive oxygen species, and transactivate the epidermal growth factor receptor in breast epithelial cells. Cancer Res 2003;63:7825–33.
34. Iida K, Itoh K, Kumagai Y, et al. Nrf2 is essential for the chemopreventive efficacy of oltipraz against urinary bladder carcinogenesis. Cancer Res 2004;64:6424–31.
35. Kohle C, Bock KW. Activation of coupled Ah receptor and Nrf2 gene batteries by dietary phytochemicals in relation to chemoprevention. Biochem Pharmacol 2006;72:795–805.
36. Wenzlaff AS, Cote ML, Bock CH, Land SJ, Schwartz AG. GSTM1, GSTT1 and GSTP1 polymorphisms, environmental tobacco smoke exposure and risk of lung cancer among never smokers: a population-based study. Carcinogenesis 2005;26:395–401.
37. Cho HY, Jedlicka AE, Reddy SP, Zhang LY, Kensler TW, Kleeberger SR. Linkage analysis of susceptibility to hyperoxia. Nrf2 is a candidate gene. Am J Respir Cell Mol Biol 2002;26:42–51.

# Enhanced Spontaneous and Benzo(*a*)pyrene-Induced Mutations in the Lung of Nrf2-Deficient *gpt* Delta Mice

Yasunobu Aoki, Akiko H. Hashimoto, Kimiko Amanuma, et al.

*Cancer Res* 2007;67:5643-5648.